Ultrasonics 96 (2019) 18–23

Contents lists available at ScienceDirect

Ultrasonics

journal homepage: www.elsevier.com/locate/ultras

Adhesive cell patterning technique using ultrasound vibrations

Kentaro Tani, Koji Fujiwara, Daisuke Koyama*

Faculty of Science and Engineering, Doshisha University, 1-3 Tataramiyakodani, Kyotanabe, Kyoto 610-0321, Japan

ARTICLE INFO

Keywords:
Cell culture
Flexural vibration
HeLa cell
Cell patterning
Cell manipulation
Acoustic radiation force

ABSTRACT

This paper investigated an ultrasound vibration cell patterning technique. The ultrasound cell culture dish consisted of a culture dish with a glass bottom and a glass disc with a piezoelectric ring that generated a resonance flexural vibration mode on the bottom of the dish. The growth of HeLa cells on the dish was observed under ultrasound excitation for 24 h. Large ultrasound vibrations on the dish inhibited the cell growth. The acoustic field was predicted with finite element analysis and it was found that the cell growth depended strongly on both the acoustic field in the culture medium and the vibration distribution of the dish. The ultrasound vibrations did not affect the viability of the cells, and the cell growth could be controlled by the flexural vibration of the cultured dish.

1. Introduction

Evaluating the physical and chemical properties of cells and tissues is important in molecular biology, and there have been many reports on in vitro cell communications [1]. Measuring the cell response to chemicals is important for the development and evaluation of new medicines and cosmetics. The group screening of cells is possible using culture dishes, flow cytometric analysis [2], and micro-patterning lab-on-a-chip techniques [3–8]. For these cell evaluations, techniques to control the growth direction and differentiation induction are essential. As a preliminary step, control of the cell culture environment and cell manipulation techniques are required, which have been achieved using chemicals [9] and magnetic beads [10]. However, use of chemicals is associated with a risk of contamination, and fabrication of the substrate with several complicated processes is required. There is a risk of cytotoxicity when using magnetic beads because they have to be attached to or introduced into cells. Although noncontact manipulation techniques for cells that allow for precise positioning using a laser beam (optical tweezers) have been proposed [11,12], these systems tend to be bulky and a large optical intensity is required.

In this paper, a method to control the cell culture using ultrasound vibrations was investigated. The noncontact ultrasound control method decreases the risk of contamination during cell culture, and the system is compact since bulky apparatus, such as mechanical actuators and light sources, are not required. There have been several reports on cell manipulation techniques using ultrasound [13–16]. Kurashina et al. reported a technique for selective detachment of adhesive cells from the culture dish using a combination of ultrasound and chemicals [17]. They proposed an efficient method to culture calf chondrocytes using trypsin and the resonance vibration mode generated on the cultivation substrate. The cultivation efficiency of the cells was improved by 20% compared with the traditional trypsin and pipetting treatment. Ding et al. reported on-chip manipulation of a single cell using a surface acoustic wave [18]. Floating cells in the microchannel were manipulated in two dimensions by controlling the acoustic standing-wave field. These manipulation techniques utilized high-frequency mechanical vibrations or the radiation force of the ultrasound, i.e., the physical ultrasound phenomena [19–22]. Here, we proposed a culture environment control technique for adherent cells using low-frequency ultrasound (tens of kHz) that enables cell patterning techniques and will be applied to control the growth direction and the differentiation induction of cells in future research. In this paper, an adhesive cell patterning technique using low-frequency ultrasound vibrations excited on the culture dish was investigated since larger vibrational amplitude can be generated at lower ultrasound frequency.

2. Materials and methods

Adhesive cells can multiply by adhering to a culture dish. The cell growth stops gradually with increasing area density and then the cells perish. In the subculture process, the proliferating cells have to be moved to other culture dishes to continue their multiplication. HeLa cells purchased from the Institute of Physical and Chemical Research, Japan, were used as adhesive cells (Fig. 1). The HeLa cells were cultured with culture medium (Eagle's minimal essential medium, Wako Pure Chemical Industries, Osaka, Japan) in an incubator with a CO_2

* Corresponding author.
E-mail address: dkoyama@mail.doshisha.ac.jp (D. Koyama).

https://doi.org/10.1016/j.ultras.2019.03.018
Received 16 October 2018; Received in revised form 11 February 2019; Accepted 27 March 2019
Available online 28 March 2019
0041-624X/

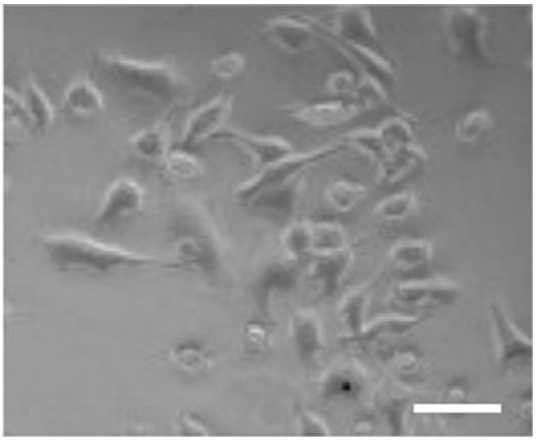

Fig. 1. Photograph of HeLa cells. The bar indicates 50 μm.

concentration of 5% and a temperature of 37 °C and then repeatedly subcultured. The culture medium was removed from the culture dish and the cells were washed with Dulbecco's phosphate-buffered saline (Nacalai Tesque, Kyoto, Japan). 1 ml of trypsin solution (Nacalai Tesque, Kyoto, Japan) was introduced to scrub the adhered cells from the culture dish, and then the culture medium was added as a buffer for the cytotoxicity of trypsin. 10 ml of the solution including the culture medium, trypsin, and the cells was centrifuged, and the cells were retrieved from the solution to be moved to other culture dishes. This subculture process was performed every three days. The viability assay using propidium iodide (PI) solution (Cosmo Bio, Tokyo, Japan) in which damaged cells are dyed red was conducted.

A cell culture dish using ultrasound vibrations was fabricated (see Fig. 2). An annular piezoelectric lead zirconate titanate (PZT) ring (inner diameter: 10 mm; outer diameter: 20 mm; thickness: 2 mm; C-213, Fuji Ceramics, Fujinomiya, Japan) polarized in the thickness direction was attached to a circular glass plate (diameter: 35 mm; thickness: 1.1 mm) by epoxy. The vibrating glass disc was in contact with the bottom of a polystyrene cell culture dish (outer diameter: 35 mm; inner diameter: 27 mm; AGC Techno Glass, Shizuoka, Japan) having a glass bottom (diameter: 30 mm; thickness: 0.18 mm) to excite the ultrasound vibrations on the bottom of the dish. Considering the disposability of the culture dish and the acoustic impedance matching between the dish and the vibrating plate, water was introduced as a coupling agent between the dish and the vibration plate so that the ultrasound vibrations could be generated efficiently on the bottom of the dish. The configurations of the piezoelectric ring and the glass plate were determined with finite element analysis (FEA) using commercial FEA software ANSYS 11.0 (ANSYS, Inc., Canonsburg, PA) to determine the resonance flexural vibration modes on the bottom of the dish. The three-dimensional simulation model included the culture medium, and the minimum element size was 0.5 mm. The vibrational distribution of the dish and the acoustic field in the culture medium was calculated from a harmonic analysis by applying a continuous sinusoidal electrical signal at the resonance frequency to the piezoelectric ring as the boundary condition.

The cultured HeLa cells with 3 ml of the culture medium were placed in the culture dish to control the liquid level height to be approximately 4 mm. The ultrasound cell culture dish was installed in a small chamber in which the temperature, humidity, and CO_2 gas density were controlled. A continuous sinusoidal electric signal from a function generator was connected to the piezoelectric ring to generate the ultrasound vibrations, and the bottom of the dish was observed with an inverted fluorescence microscope (IX83, Olympus, Tokyo, Japan) under ultrasound excitation for 24 h. The vibration distribution on the dish without culture medium was measured by a laser Doppler vibrometer (LDV; NLV-2500, PI Polytec, Waldbronn, Germany) since the reflected light at the medium surface interfered with the observational signal.

3. Results and discussion

There were several resonance frequencies of the ultrasound cell culture dish over 20 kHz, and, in this paper, the resonance flexural vibration mode of 83 kHz was used. Fig. 3(a) shows the out-of-plane vibrational displacement amplitude distribution of the dish. The 27 × 27 mm^2 area at the center of the bottom of the dish was scanned, and the result was normalized by the maximum value. Fig. 3(b) shows

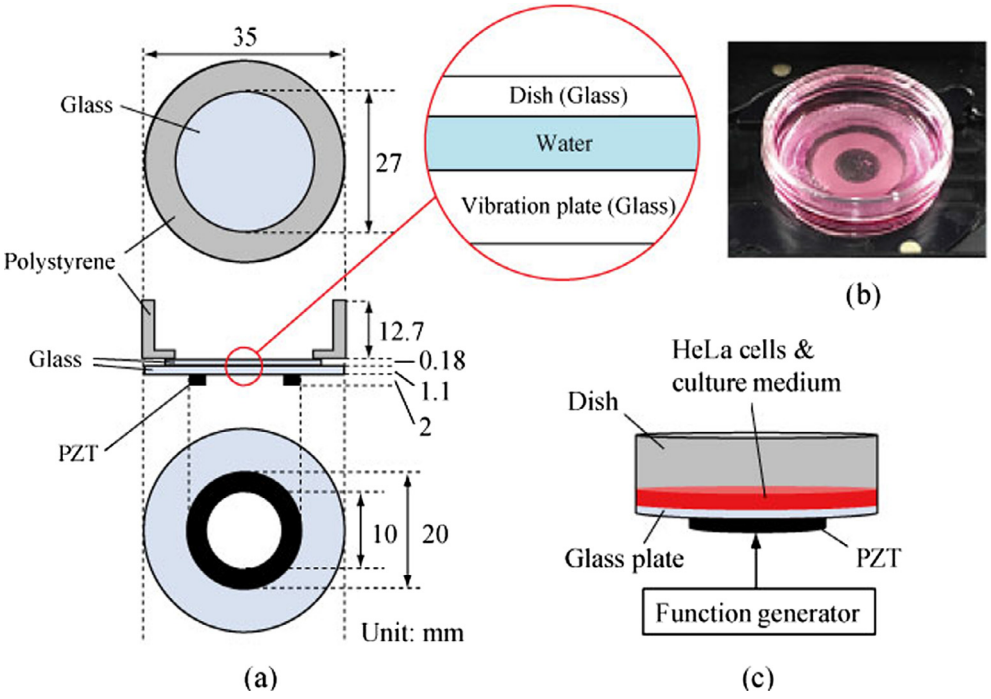

Fig. 2. (a) Configuration and (b) photograph of an ultrasound cell culture dish. (c) Observation system for the cell culture.

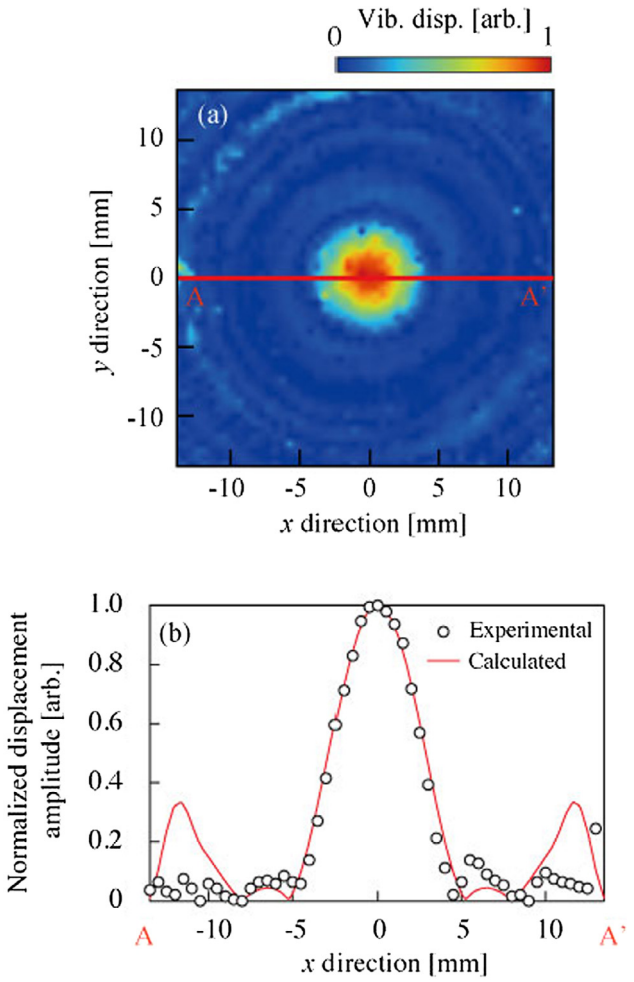

Fig. 3. (a) Vibration distribution on the bottom of the culture dish at 78 kHz and (b) the radial profile along line A-A′.

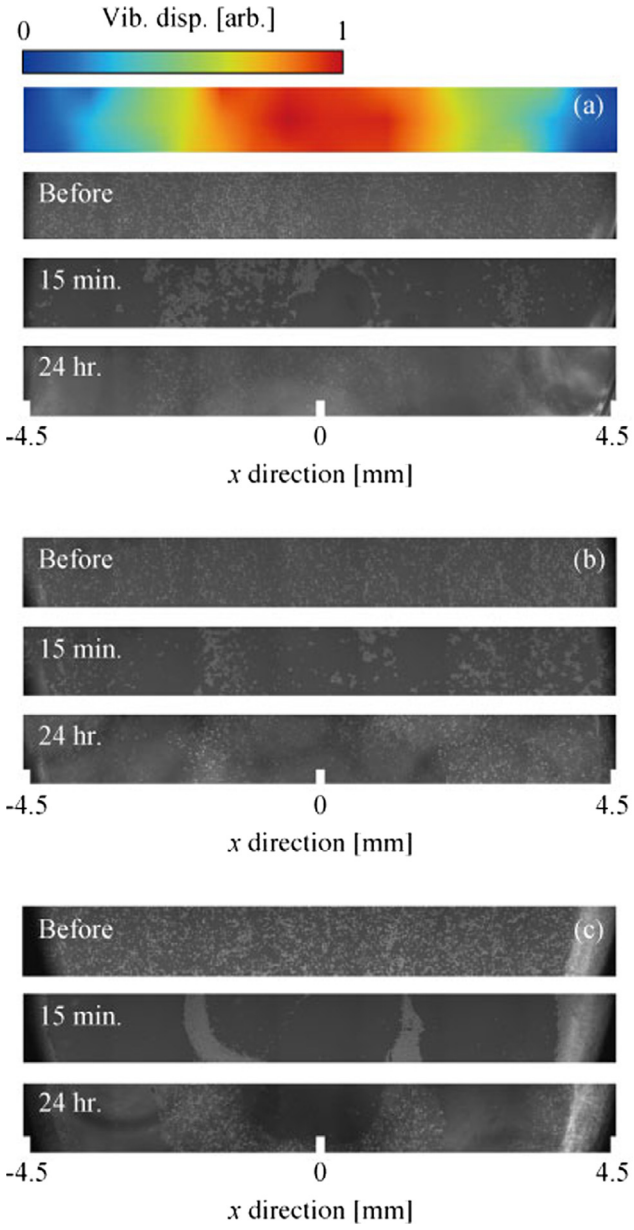

Fig. 4. Sequential microscopic phase-contrast images of the HeLa cells on the culture dish excited with (a) 5 V_{pp} (and the vibrational distribution of the dish), (b) 7 V_{pp}, and (c) 10 V_{pp}. The cells appear bright.

the radial profile along line A-A′, and the calculated FEA result is also shown. The experimental and calculated FEA results showed good agreement. The vibration amplitude was largest at the center of the dish, and the axisymmetric resonance flexural vibration mode with three concentric nodal circles and no nodal line was generated on the bottom of the dish. In the cases of higher (or lower) resonance frequencies, a larger (or smaller) number of vibration nodal circles and lines appeared.

The effect of ultrasound vibrations on the cell multiplication was examined. Fig. 4 shows photographs of the HeLa cells in the culture medium before ultrasound excitation, after 15 min of excitation, and 24 h of excitation with the input voltages of 5 V_{pp}, 7 V_{pp}, and 10 V_{pp}. A $9 \times 1\ mm^2$ area around the center of the dish was scanned in the x-direction by the microscope. The experimental result of the vibration distribution of the dish in the same area was also shown for comparison. The photographs were taken by phase-contrast imaging and the cells appeared brighter compared with the background under the microscopic view. Before ultrasound excitation, the HeLa cells were distributed uniformly over the whole observation range. By generating ultrasound vibrations on the dish, the cells were aggregated at two positions at around $x = \pm 1.7$ mm after 15 min (specifically, they were on the circumference of circle with a radius of 1.7 mm), and this tendency was enhanced with increased input voltage (Fig. 4(c)). After 24 h of ultrasound excitation, the cells multiplied from the position where they were aggregated. The cells were distributed over the whole cultured dish when the input voltages were 5 V_{pp} and 7 V_{pp}. However, when the input voltage was increased to 10 V_{pp}, the cell growth area was limited and the cells did not multiply toward the center of the culture dish. The results indicated that the cell growth could be controlled by the ultrasound flexural vibration and this effect was enhanced by increasing the input voltage to the piezoelectric ring.

The relationship between the cell growth and the ultrasound vibrations was investigated. The cell growth was evaluated by the average brightness of the microscopic images, which was calculated every 0.25 mm in the x-direction ($0.25 \times 1\ mm^2$ area). Fig. 5 shows the distributions of the vibrational displacement amplitude of the dish and the brightness of the microscopic images in Fig. 4. The brightness was normalized by the maximum value from $x = -4$ mm to 4 mm in each microscopic image. A flexural vibration with a 10 mm half wavelength was generated at the center of the dish and the nodal positions corresponded to $x = \pm 5$ mm. The displacement amplitude was proportional to the input voltage; the maximal vibration amplitude at the center was 0.4 μm when the input voltage was 10 V_{pp}. When the input voltage was 5 V_{pp} and 7 V_{pp} (Fig. 5(a) and (b), respectively), the distributions of the

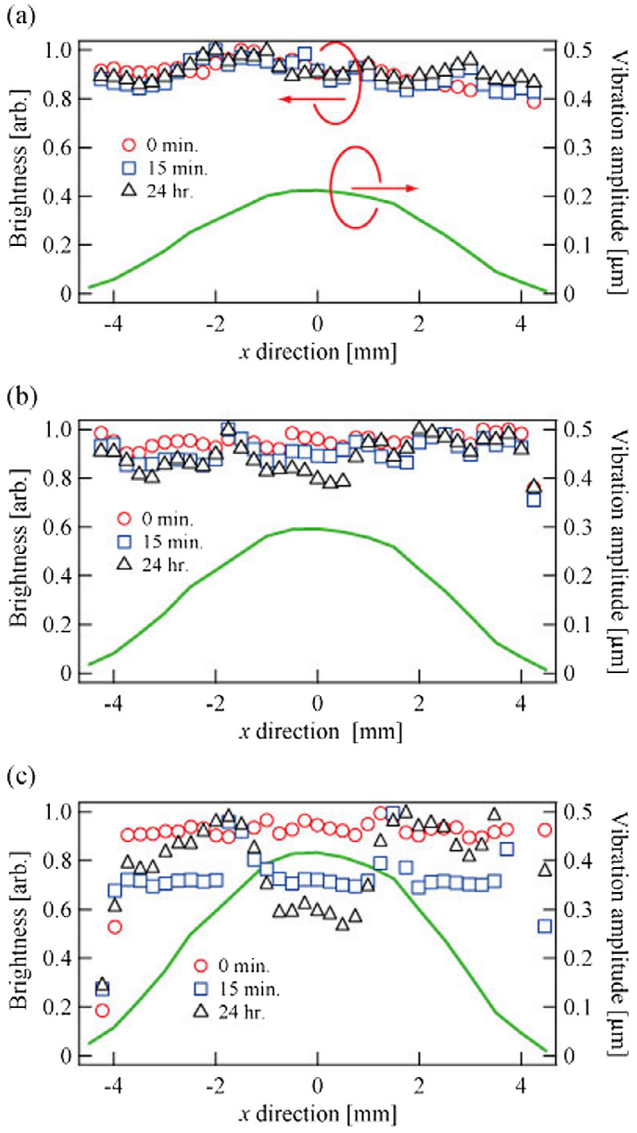

Fig. 5. Distributions of the brightness of the microscopic images (plots) and the vibration amplitude distributions (solid lines) on the culture dish excited with (a) 5 V_{pp}, (b) 7 V_{pp}, and (c) 10 V_{pp}.

image brightness in the x-direction were roughly uniform, and changed little with the passage of time. When the input voltage was increased to 10 V_{pp} (Fig. 5(c)), the brightness increased relatively at x = ± 1.7 mm and decreased around the center (x = 0 mm) after 15 min. In addition, the brightness decrease at the center was enhanced after 24 h, and this means that the multiplication of HeLa cells was inhibited by large ultrasound vibrations. It is known that small particles on an ultrasound vibrating plate are aggregated and aligned along the nodal line of a standing wave (the phenomenon is termed Chladni's figure) [23]. However, the positions where the cells were aggregated and grew did not correspond with the nodal circles of the ultrasound flexural vibration excited on the cultured dish.

Another important factor is the acoustic field in the culture medium. The resonance modes of an acoustic field are generated in a thin cavity and are determined from the relationships among the configuration of the cavity, the speed of sound in the medium, and the ultrasound frequency [24]. This means that the sound pressure distribution does not necessarily correspond with the vibration distribution of the plate. The acoustic field in the culture medium was calculated by the FEA at 83 kHz, and the acoustic radiation force in an acoustic standing wave acting on a small rigid sphere was predicted from the sound pressure

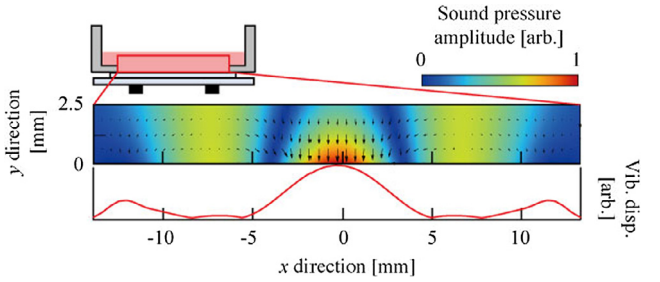

Fig. 6. Sound pressure amplitude distribution, the vector flow of the acoustic radiation force in the culture medium just above the bottom of the dish, and the vibration distribution on the dish.

amplitude distribution [25–28]. The acoustic radiation force on a small rigid sphere in an acoustic standing wave field F can be expressed as [27]

$$F = VD\nabla\overline{K_E} - V(1-\gamma)\nabla\overline{P_E}, \tag{1}$$

$$D = \frac{3(\rho - \rho_0)}{2\rho + \rho_0}, \tag{2}$$

where V is the volume of the rigid sphere, ρ is the density of the sphere, ρ_0 is the density of the medium, γ is the ratio of the compressibility of the medium to that of the sphere, K_E is the time-averaged kinetic energy, $\overline{P_E}$ is the time-averaged potential energy, and ∇ is the gradient operator. The kinetic energy K_E and the potential energy P_E are expressed as

$$K_E = \frac{1}{2}\rho_0 v^2, \tag{3}$$

$$P_E = \frac{1}{2}\cdot\frac{p^2}{\rho_0 c^2}, \tag{4}$$

where v ($=j/\omega\rho_0\cdot\mathrm{grad}\,p$) is the particle velocity, c is the speed of sound in the medium, ω is the angular frequency, and p is the sound pressure. Fig. 6 shows the sound pressure amplitude distribution and the vector flow of the acoustic radiation force in the culture medium just above the bottom of the dish. For comparison, the vibration distribution on the bottom of the dish shown in Fig. 3(b) is also shown. An acoustic standing wave with the nodal circle with a radius of approximately 3 mm was generated at the center of dish. Therefore the cells will be attracted to the nodal circle of the sound pressure (x = ± 3 mm), which is smaller than that of the flexural vibration of the dish (x = ± 5 mm) since a rigid particle that is much smaller than the wavelength of the ultrasound is attracted and trapped at the nodal points of the sound pressure amplitude in a standing-wave field [29]. It should be noted that the acoustic radiation force acted toward the bottom surface of the dish, enabling the HeLa cells to attach to the bottom so that they can multiply. In fact, the focus point of the microscopic images in Fig. 3 was constant and corresponded to the bottom surface, indicating that the cells were constantly aggregated just above the bottom surface of the dish.

Although there are several methods to measure the sound pressure amplitude in a thin layer including a needle hydrophone, an LDV [30], and fiber optic sensors [31], the acoustic field in the culture medium was visualized using small particles to investigate the relationship between the acoustic field and the cell growth. Silica microspheres with an average diameter of 25 μm were scattered on the culture dish with no cells. Fig. 7 shows the microscopic image of the microspheres trapped in the acoustic standing wave in the culture medium. The microspheres were trapped instantaneously and statically at the positions around x = ± 1.7 mm where the cells existed after 15 min (Fig. 4(c)), not the nodal positions of the flexural vibration generated on the dish. The difference in the experimentally observed and predicted trapped positions can be attributed to the material properties used in the FEA;

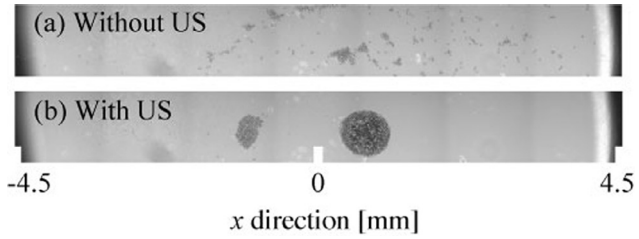

Fig. 7. Microscopic images of silica microspheres on the culture dish (a) without and (b) with ultrasound excitation.

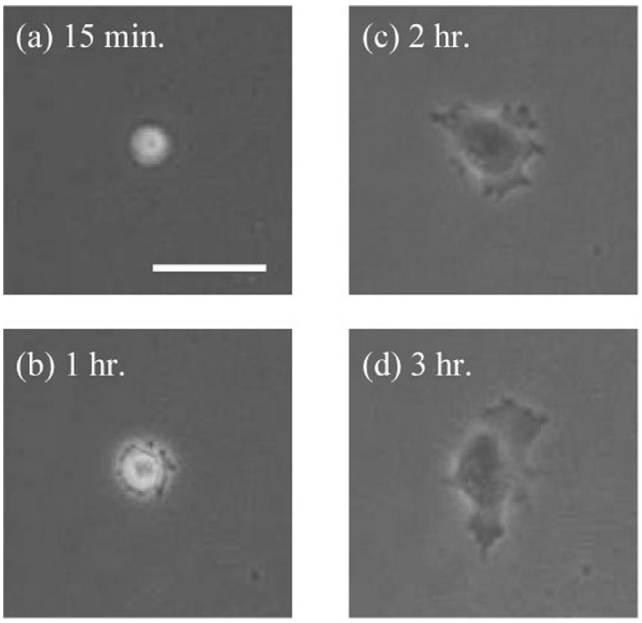

Fig. 8. Sequential microscopic images of the HeLa cell on the culture dish under ultrasound excitation. Bar indicates 50 μm.

the speed of sound in the medium was assumed to be 1.5×10^3 m/s. From the experimental result, we can explain the changes in the cell growth shown in Figs. 4 and 5 as follows. The cells in the culture medium placed on the dish did not adhere to the bottom of the dish instantaneously and were aggregated to the nodal points of the acoustic standing wave just over the bottom of the dish by the acoustic radiation force. The cells gradually adhered to the dish over time at the position where they were trapped and then multiplied outward on the dish. In fact, the area densities of the cells at x = ± 1.7 mm were temporarily increased (15 min in Fig. 4(c)) and then decreased (24 h in Fig. 4(c)). Fig. 8 shows the sequential microscopic images of one of the cells under ultrasound excitation. The HeLa cell appeared spherical after 15 min when it had not yet adhered to the dish but after 1 h it changed its profile to adhere and multiply. This means that the cells were aggregated tightly next to each other by the acoustic radiation force after 15 min and then the area density decreased, because there is a threshold of the area density for the cell multiplication [32]. Compared with previously reported cell manipulation techniques using MHz-range ultrasound, the acoustic radiation force to the HeLa cells is relatively small since the intensity of the acoustic radiation force depends on the relationship between the cell size and the ultrasound wavelength; the wavelength of tens-kHz-range ultrasound (tens mm) is much larger than the cell size (tens μm) and higher ultrasound frequency with shorter wavelength (hundreds μm) in MHz-range is suitable for the acoustic manipulation. It should be noted that the cells did not grow toward the center of the dish where the sound pressure amplitude and the vibration amplitude of the dish were large, and this is because cell adhesion on the substrate can be scrubbed by large vibration amplitudes [17].

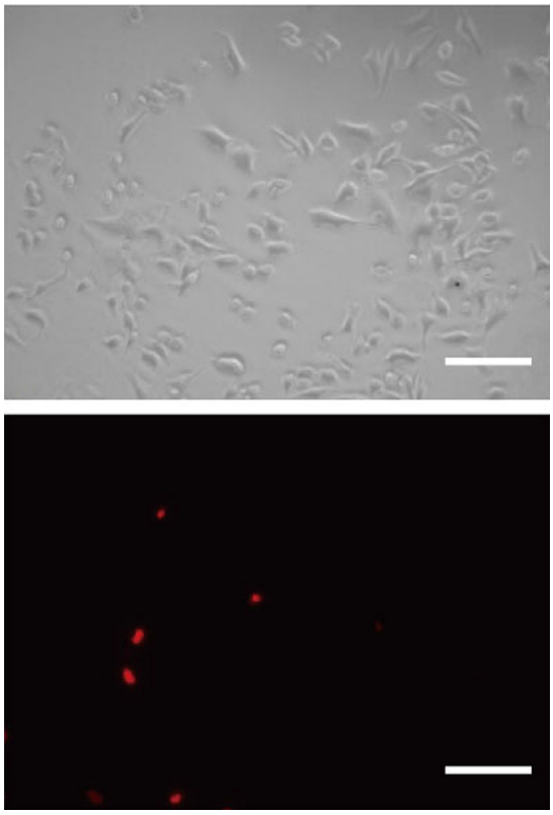

Fig. 9. (a) Microscopic phase-contrast and (b) fluorescent images of the HeLa cells after ultrasound excitation for 30 s. Bar indicates 100 μm.

Therefore, the area of the cell growth strongly depends on both the acoustic field in the culture medium and the vibration distribution of the dish, and the cell growth on the culture dish could be controlled by ultrasound vibrations.

The viability assay using the PI solution was conducted to evaluate the effect of ultrasound vibrations on the cultured cells. Fig. 9 shows the representative phase contrast and fluorescent images of the HeLa cells after ultrasound excitation for 30 s. Under the fluorescent microscopic view, the dead cells were red since the PI solution can penetrate through the damaged cell membrane. Fig. 10 shows the relationship between the input voltage to the piezoelectric ring and the ratio of dead cells. The plots and error bars express the average values and four standard deviations. Acoustic cavitation generated by low-frequency ultrasound, which could damage the cell, was not observed in these experimental conditions. Compared with the control (0 V_{pp}), the ratio of dead cell showed little change the input voltage increased from 2 V_{pp}

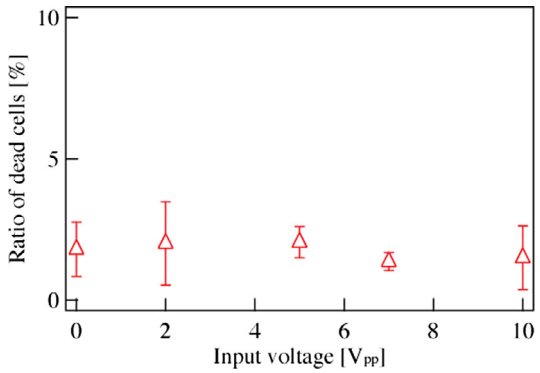

Fig. 10. Relationship between the input voltage to the piezoelectric ring and the rate of dead cells.

to 10 V_{pp}; the ratios were approximately 2% in all cases. This result indicates that the ultrasound vibrations and the sound pressure did not affect the viability of HeLa cells under these conditions.

4. Conclusions

The ultrasound vibration cell patterning technique was investigated. A disposable ultrasound culture dish was fabricated, and the growth of HeLa cells was evaluated. The cell growth depended strongly on both the acoustic field in the culture medium and the vibrational distribution generated on the bottom of the dish, and the cell patterning could be controlled by switching the resonance vibration mode. It was confirmed that the ultrasound vibrations did not affect the cell viability under these experimental conditions. One of the advantages of this technique is that positions where cells are trapped can be controlled easily by changing the resonance vibration mode of the dish. For future application of this technique such as an evaluation of cell communication, the vibration mode of a culture dish should be modified to lattice flexural modes so that cells can be arranged with same intervals in a two-dimensional plane.

Acknowledgments

This work was partially supported by a bilateral program from the Japan Society for the Promotion of Science (JSPS) and the MEXT supported program for the strategic research foundation at private universities 2013-2018. We thank Melissa Gibbons, PhD, from Edanz Group (www.edanzediting.com/ac) for editing a draft of this manuscript.

References

[1] O. Shaya, U. Binshotok, M. Hersch, D. Rivkin, S. Weinreb, L. Amir-Zilberstein, B. Khamaisi, O. Oppenheim, R. Desai, R. Goodyear, G. Richardson, C. Chen, D. Sprinzak, Cell-cell contact area affects Notch signaling and Notch-dependent patterning, Dev. Cell 40 (5) (2017) 505–511.
[2] I. Nicoletti, G. Migliorati, M. Pagliacci, F. Grignani, C. Riccardi, A rapid and simple method for measuring thymocyte apoptosis by propidium iodide staining and flow cytometry, J. Immunol. Methods 139 (2) (1991) 271–279.
[3] M. Hahn, L. Taite, J. Moon, M. Rowland, K. Ruffino, J. West, Photolithographic patterning of polyethylene glycol hydrogels, Biomaterials 27 (12) (2006) 2519–2524.
[4] S. Nagrath, L. Sequist, S. Maheswaran, D. Bell, D. Irimia, L. Ulkus, M. Smith, E. Kwak, S. Digumarthy, A. Muzikansky, P. Ryan, U. Balis, R. Tompkins, D. Haber, M. Tone, Isolation of rare circulating tumour cells in cancer patients by microchip technology, Nature 450 (2007) 1235–1239.
[5] Y. Huang, B. Rubinsky, Flow-through micro-electroporation chip for high efficiency single-cell genetic manipulation, Sens. Actuat. A Phys. 104 (3) (2013) 205–212.
[6] K. Morishima, T. Fukuda, F. Arai, K. Yoshikawa, Transportation of DNA molecule by dielectrophoretic force in micro flow channel -Utilization of conformational transition in the higher order structure of DNA, Proc. Seventh International Symposium on Micro Machine and Human Science, 1996, pp. 171–176.
[7] A. Bhagat, H. Bow, H. Hou, S. Tan, J. Han, C. Lim, Microfluidics for cell separation, Med. Biol. Eng. Comput. 48 (10) (2010) 999–1014.
[8] C. Yi, C. Li, S. Ji, M. Yang, Microfluidics technology for manipulation and analysis of biological cells, Anal. Chim. Acta 560 (1–2) (2006) 1–23.
[9] N. Alves, I. Pashkuleva, R. Reis, J. Mano, Controlling cell behavior through the design of polymer surfaces, Small 6 (20) (2010) 2208–2220.
[10] V. Sivagnanam, B. Song, C. Vandevyver, J. Bünzli, M. Gijs, Selective breast cancer cell capture, culture, and immunocytochemical analysis using self-assembled magnetic bead patterns in a microfluidic chip, Langmuir 26 (9) (2010) 6091–6096.
[11] A. Mizuno, M. Nishioka, T. Tanizoe, S. Katsura, Handling of single DNA molecule using electric field and laser beam, IEEE Trans. Appl. Ind. 31 (6) (1995) 1452–1457.
[12] H. Zhang, K. Liu, Optical tweezers for single cells, J. R. Soc. Interface 5 (24) (2008) 671–690.
[13] F. Guo, Z. Mao, Y. Chen, Z. Xie, J. Lata, P. Li, L. Ren, J. Liu, J. Yang, M. Dao, S. Suresh, T. Huang, Three-dimensional manipulation of single cells using surface acoustic waves, Proc. Natl. Acad. Sci. USA 113 (6) (2015) 1522–1527.
[14] A. Nawaz, Y. Chen, N. Nama, R. Nissly, L. Ren, A. Ozcelik, L. Wang, J. McCoy, S. Levine, T. Huang, Acoustofluidic fluorescence activated cell sorter, Anal. Chem. 87 (24) (2015) 12051–12058.
[15] D. Ahmed, A. Ozcelik, N. Bojanala, N. Nama, A. Upadhyay, Y. Chen, W. Hanna-Rose, T. Huang, Rotational manipulation of single cells and organisms using acoustic waves, Nat. Commun. 7 (2016) 11085.
[16] H. Mulvana, S. Cochran, M. Hill, Ultrasound assisted particle and cell manipulation on-chip, Adv. Drug Deliv. Rev. 65 (11–12) (2013) 1600–1610.
[17] Y. Kurashina, K. Takemura, J. Friend, S. Miyata, J. Komotori, Efficient subculture process for adherent cells by selective collection using cultivation substrate vibration, IEEE Trans. Biomed. Eng. 64 (3) (2016) 580–587.
[18] X. Ding, S. Lin, B. Kiraly, H. Yue, S. Li, I. Chiang, J. Shi, S. Benkovic, T. Huang, On-chip manipulation of single microparticles, cells, and organisms using surface acoustic waves, Proc. Natl. Acad. Sci. USA 109 (28) (2012) 11105–11109.
[19] A.L. Bernassau, F. Gesellchen, P.G.A. MacPherson, M. Riehle, D.R.S. Cumming, Direct patterning of mammalian cells in an ultrasonic heptagon stencil, Biomed. Microdevices 14 (3) (2012) 559–564.
[20] D.J. Collins, B. Morahan, J. Garcia-Bustos, C. Doerig, M. Plebanski, A. Neild, Two-dimensional single-cell patterning with one cell per well driven by surface acoustic waves, Nat. Commun. 6 (2015) 8686.
[21] F. Gesellchen, A.L. Bernassau, T. Déjardin, D.R.S. Cumming, M.O. Riehle, Cell patterning with a heptagon acoustic tweezer–application in neurite guidance, Lab Chip 14 (13) (2014) 2266–2275.
[22] J. Shi, D. Ahmed, X. Mao, S. Lin, A. Lawit, T. Huang, Acoustic tweezers: patterning cells and microparticles using standing surface acoustic waves (SSAW), Lab Chip 9 (20) (2009) 2890–2895.
[23] R. Kashima, D. Koyama, M. Matsukawa, Two-dimensional noncontact transportation of small objects in air using flexural vibration of a plate, IEEE Trans. Ultrason., Ferroelect., Freq. Contr. 62 (12) (2015) 2161–2168.
[24] D. Koyama, Y. Wada, K. Nakamura, M. Nishikawa, T. Nakagawa, H. Kihara, An ultrasonic air pump using an acoustic traveling wave along a small air gap, IEEE Trans. Ultrason., Ferroelect., Freq. Contr. 57 (1) (2010) 253–261.
[25] G. Maidanik, Acoustic radiation pressure due to incident plane progressive waves on spherical objects, J. Acoust. Soc. Am. 29 (6) (1957) 738–742.
[26] T. Hasegawa, K. Yosioka, Acoustic-radiation force on a solid elastic sphere, J. Acoust. Soc. Am. 46 (5B) (1969) 1139–1143.
[27] W.L. Nyborg, Physical principles of ultrasound, Ultrasound: its Applications in Medicine and Biology Amsterdam, Elsevier Scientific Publishing Company, The Netherlands, 1978, p. 52.
[28] D. Koyama, K. Nakamura, Noncontact ultrasonic transportation of small objects over long distances in air using a bending vibrator and a reflector, IEEE Trans. Ultrason., Ferroelect., Freq. Contr. 57 (5) (2010) 1152–1159.
[29] A. Haake, J. Dual, Positioning of small particles by an ultrasound field excited by surface waves, Ultrasonics 42 (1-9) (2004) 75–80.
[30] S. Sato, Y. Wada, D. Koyama, K. Nakamura, Estimation of absolute sound pressure in a small-sized sonochemical reactor, Ultrasonics Sonochem. 20 (1) (2013) 468–471.
[31] H. Takei, D. Koyama, K. Nakamura, S. Ueha, Air flow in a small gap between a bending vibrator and a reflector, Jpn. J. Appl. Phys. 47 (5) (2008) 4276–4281.
[32] P. Hung, P. Lee, P. Sabounchi, R. Lin, L. Lee, Continuous Perfusion microfluidic cell culture array for high-throughput cell-based assays, Biotechnol. Bioeng. 89 (1) (2005) 1–8.